Pharmaceutical Development and Technology

ISSN: 1083-7450 (Print) 1097-9867 (Online) Journal homepage: http://www.tandfonline.com/loi/iphd20

Diloxanide furoate binary complexes with β-, methyl-β-, and hydroxypropyl-β-cyclodextrins: inclusion mode, characterization in solution and in solid state and in vitro dissolution studies

Carolina Aloisio & Marcela Longhi

To cite this article: Carolina Aloisio & Marcela Longhi (2017): Diloxanide furoate binary complexes with β-, methyl-β-, and hydroxypropyl-β-cyclodextrins: inclusion mode, characterization in solution and in solid state and in vitro dissolution studies, Pharmaceutical Development and Technology, DOI: 10.1080/10837450.2017.1362435

To link to this article: http://dx.doi.org/10.1080/10837450.2017.1362435

Accepted author version posted online: 31 Jul 2017.
Published online: 16 Aug 2017.

PHARMACEUTICAL DEVELOPMENT AND TECHNOLOGY, 2017
https://doi.org/10.1080/10837450.2017.1362435

Taylor & Francis
Taylor & Francis Group

RESEARCH ARTICLE

Diloxanide furoate binary complexes with β-, methyl-β-, and hydroxypropyl-β-cyclodextrins: inclusion mode, characterization in solution and in solid state and *in vitro* dissolution studies

Carolina Aloisio and Marcela Longhi

CONICET and Departamento de Farmacia, Facultad de Ciencias Químicas, Unidad de Investigación y Desarrollo en Tecnología Farmacéutica (UNITEFA), Universidad Nacional de Córdoba, Ciudad Universitaria, Córdoba, Argentina

ABSTRACT

The purpose of this study was to investigate the effect on solubility and dissolution rate of binary complexes of β-(βCD), methyl-(MβCD) and hydroxypropyl-β-cyclodextrin (HPβCD) with diloxanide furoate (DF). The complexation in solution was evaluated by phase solubility studies and ^{1}H nuclear magnetic resonance (NMR). Enhanced water solubility of DF was obtained with the DF:MβCD system (61-fold). The mode of inclusion was supported by NMR experiments, which indicated that real inclusion complexes were formed between DF and MβCD or HPβCD. Solid state analysis was performed using infrared and thermal methods, which suggested the formation of true inclusion complexes of DF with two derivatized cyclodextrins, MβCD and HPβCD, and an exclusion complex with βCD when the systems were prepared by freeze-dried technique. Dissolution studies conducted in simulated gastric fluid (2 h) and subsequent simulated intestinal fluid (next 4 h) showed increased dissolution rate of DF from the freeze-dried systems with βCD, MβCD, and HPβCD (85; 77 and 75% of dissolved drug at 5 min, respectively) and 100% of the drug dissolved at 150 min for the three systems. The enhancement of the solubility and the dissolution of DF observed make these complexes promising candidates for the preparation of oral pharmaceutical formulations.

ARTICLE HISTORY
Received 20 February 2017
Revised 3 May 2017
Accepted 28 July 2017

KEYWORDS
Diloxanide furoate; cyclodextrin; complexation; mode of interaction; solid state characterization; *in vitro* dissolution

1. Introduction

Pathogenic intestinal protozoa are responsible for clinically important infections in both the developed and the developing world. Amoebiasis affects around 480 million people worldwide, with an annual mortality of 40 000–110 000 persons. These organisms are responsible for both acute and chronic diarrhea, and *Entamoeba histolytica*, which affects the colon, can spread to involve the liver. Acute amebic colitis ranges from mild to severe, and can be fulminant, leading to colon perforation. The infection can spread from the liver by direct extension into the pleuropulmonary cavity and the pericardial cavity. Occasionally, and most often in immuno-suppressed individuals, the infection might be widely disseminated and affect other organs, including bones and the brain (Farthing 2006). Diloxanide furoate (DF) (Figure 1(a)) is one of the drugs of choice for the treatment of amebic colitis caused by Entamoeba histolytica (Budal et al. 2004; Mishal and Sober 2005; Farthing 2006). DF acts on organisms in the intestinal lumen (Farthing 2006). For this reason, high concentrations of this drug in the intestinal fluids are substantially related to the effectiveness of the drug. Orally administered drugs must have sufficient water solubility to ensure their bioavailability and pharmacological activity (Ojarinta et al. 2017). However, DF presents little solubility in water, which can affect its action against *Entamoeba histolytica* (Budal et al. 2004). Accordingly, the use of suitable strategies to increase water solubility of DF and dissolution rate in the intestinal fluids may reduce the possibility of the drug precipitating in the lumen, and this would lead to a loss in effectiveness.

Cyclodextrins (CD) are cyclic oligosaccharides containing at least 6D (+) glucopyranose units attached by (1–4) glucosidic bonds. These cyclic glucopyranose molecules form a truncated cone with a lipophilic inner cavity and a hydrophilic outer surface (Taupitz et al. 2013). CD are known to form inclusion complexes with a variety of guest molecules in both solution and solid state, which is successfully utilized for the improvement of pharmaceutical properties of drugs (Ribeiro et al. 2003; Araújo et al. 2008). It is well described in the literature that CD can be used as solubilizing agents for drugs presenting a poor aqueous solubility (Barillaro et al. 2007). However, the poor water solubility of native CD, especially βCD, and their complexes led to the preparation of more water-soluble derivatives through chemical modifications. For instance, the random substitution of any of the hydroxyl group bonds in the positions C-2, C-3, and C-6, by hydrophobic moieties, has resulted in significant increases in their aqueous solubility and capacity of inclusion, while they have a favorable toxicological profile (Veiga et al. 2006; Duchêne and Bochot 2016). Complexes of these βCD derivatives, such as the methylated βCD (MβCD) and hydroxypropylated βCD (HPβCD) (Figure 1(b)) (Kutyła et al. 2013) with drug molecules exhibit different properties from their original free forms and usually result in enhancement of aqueous solubility (Granero et al. 2008; Aloisio et al. 2014), better chemical stability (Garnero and Longhi 2007; Zoppi et al. 2011) and increased permeability and bioavailability of the drugs (Yi et al. 2009; Özdemir and Erkin 2012). Previously, Budal et al. studied the inclusion complex of DF with CD. It is worth mentioning that they only described the effect of βCD on DF solubility by phase solubility diagrams at pH 7. Besides,

CONTACT Marcela Longhi mrlcor@fcq.unc.edu.ar CONICET and Departamento de Farmacia, Facultad de Ciencias Químicas, Unidad de Investigación y Desarrollo en Tecnología Farmacéutica (UNITEFA), Universidad Nacional de Córdoba, Ciudad Universitaria, Córdoba, Argentina

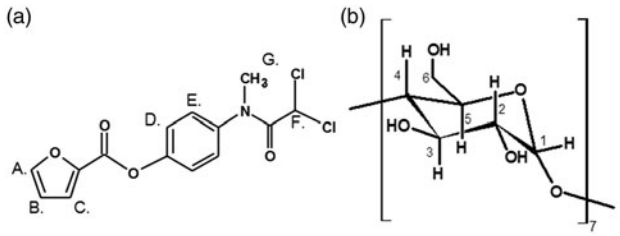

Figure 1. Chemical structure of: (a) diloxanide furoate; (b) βCD, MβCD, or HPβCD when R = H; $-CH_3$ or $-CH_2CH(OH)CH_3$, respectively.

it is worth highlighting that aqueous solubility determinations may not provide a sufficiently comprehensive perspective of the dissolution behavior of a drug in the gastrointestinal tract, since there are numerous factors, such as differences in pH, which may influence the dissolution process (Ojarinta et al. 2017). To overcome this challenge, dissolution rate studies utilizing solutions that simulate gastric or intestinal fluids, and which are easy to prepare in the laboratory, have been introduced (Ojarinta et al. 2017). Budal et al. also mentioned that ^{1}H NMR and ^{13}C were used to characterize DF:βCD inclusion complexes, but finally declared that the sensitivity of their NMR equipment (a BRUKER model AC300 spectrophotometer) was not high enough to detect complexation in the experimental conditions used. Besides, some experiments were carried out in solvent mixtures (water–methanol and water–acetonitrile), but these more hydrophobic environments hindered complexation (Budal et al. 2004). In addition, MβCD and HPβCD interactions with DF were not determined so far, and no solid state characterization of any DF:CD complex was yet described. On the other hand, Castro et al. indicated that the efficacy against *Cryptosporidium parvum* of a βCD:DF 'inclusion complex', prepared by kneading, was evaluated in a suckling murine model; and Blanco et al. prepared DF-loaded microspheres containing βCD and MβCD in order to improve the drug solubilization in water to facilitate the microspheres elaboration procedure (Castro Hermida et al. 2001; Blanco-García et al. 2016). However, no characterization studies that confirm the formation of a true inclusion complex were presented in any of these works in regard toF:CD complexes.

From this basis, the present work was conducted to evaluate the formation of binary systems with βCD, MβCD, and HPβCD, and to determine the mode of interaction of the complexes by nuclear magnetic resonance (NMR) spectroscopy. Besides, solid state characterization of DF:CD complexes by Fourier-transform infrared spectroscopy (FT-IR) and thermal analysis [differential scanning calorimetry (DSC) and thermogravimetric analysis (TGA)] was performed. In addition, the dissolution profiles of DF complexes with βCD, MβCD, and HPβCD in simulated gastrointestinal tract fluids were obtained.

2. Methods

2.1. Materials

Diloxanide furoate was obtained from Parafarm®, Argentina. βCD ($M_W = 1135$), MβCD ($M_W = 1190$), and HPβCD ($M_W = 1325$) were kindly supplied by Ferromet® (Roquette®'s agent in Argentina). All the other materials and solvents were of analytical reagent grade. A Millipore Milli-Q Water Purification System generated the water used in these studies.

2.2. Phase solubility studies (PSS)

Solubility diagrams were obtained according to Higuchi and Connors method (Higuchi and Connors 1965). Each experiment was performed in triplicate. Excess amounts of DF, for saturation conditions, were added to aqueous or buffered solutions containing βCD (0–16 mM), MβCD (0–100 mM), or HPβCD (0–28 mM), in relation with their aqueous solubility. The suspensions formed were sonicated in an ultrasonic bath for 15 min every 12 h to favor solubilization and then placed in a 25.0 ± 0.1 °C constant temperature bath [HAAKE DC10 thermostat (Haake®, Paramus, NJ)] for 72 h. After equilibrium was reached, the suspensions were filtered through a 0.45 μm membrane filter (Millipore®, Billerica, MA) and analyzed in a Shimadzu® UV-160 (Kyoto, Japan) spectrophotometer. The equilibrium pH of each solution was measured (Hanna® HI 255 pH-meter, Woonsocket, RI). The apparent stability constants ($K_{1:1}$) of the DF:CD complexes were determined as a function of the added ligand concentration ([CD]) (Granero et al. 2008). Since the phase solubility diagrams were A-type and assuming a 1:1 complex at low concentrations of ligand, the apparent stability (or formation) constants $K_{1:1}$ were calculated using the slope from the linear regression analysis of the first portion of the phase solubility isotherms using the following equation:

$$K_c = \text{slope}/S_0\,(1 - \text{slope}) \quad (1)$$

where S_0 is the solubility of the pure drug.

In addition, complexation efficiency (CE) was calculated from the slope of phase-solubility diagrams (Piel et al. 2006):

$$CE = S_0 \,.\, K_c \quad (2)$$

2.3. Nuclear magnetic resonance studies

^{1}H NMR studies were performed at 298 K in a Bruker® Avance II High Resolution Spectrometer equipped with a Broad Band Inverse (BBI) probe and a Variable Temperature Unit (VTU) using 5 mm sample tubes. Spectra were obtained at 400.16 MHz. Based on the 1:1 stoichiometry data obtained in the PSS, complexes and pure substance solutions were prepared in D_2O, and for the complex incorporating an excess amount of the drug with a fixed concentration of each ligand; these were sonicated for an hour to favor the maximum DF solubilization so as to obtain a measurable concentration of the drug and to form the complexes. The suspensions were filtered before their analysis. The NMR data were processed with the Bruker TOPSPIN 2.0 software (Billerica, MA). The residual solvent signal (4.80 ppm) was used as the internal reference. Induced changes in the ^{1}H NMR chemical shifts ($\Delta\delta$) for DF, originated due to their interaction with the ligands, were calculated according to the following equation:

$$\Delta\delta = \delta \text{ complex} - \delta \text{ free} \quad (3)$$

2.4. Solid sample preparation

Freeze-dried systems (FDS) were obtained by the freeze-drying technique using Labconco® Freeze Dye 4.5 equipment (Kansas City, MO), at −48 ± 1 °C with 50 mbar vacuum for 36 h. Based on the 1:1 stoichiometry data obtained in the PSS, equimolar ratio complexes of binary systems and pure substance aqueous solutions were prepared by incorporating an excess amount of the drug with a fixed concentration of each ligand which was sonicated for two hours. The suspensions were filtered and then frozen at −40 °C up to their complete solidification for the freeze-drying procedure. On the other hand, physical mixtures (PM) of the components were prepared using the same molar ratios, by simple mixing in agate mortar.

2.5. Fourier-transform infrared spectroscopy

The FT IR spectra of pure substances, FDS and PM were recorded as potassium bromide discs using a Nicolet 5 SXC FT IR spectrometer (Eagle River, WI). The signal changes of the corresponding functional groups were compared to analyze the mode of interaction between them.

2.6. Differential scanning calorimetry, thermogravimetric analysis, and derivative thermogravimetric analysis (DTG)

The thermal behavior of the drug and complexes were studied by heating the samples in pierced aluminum-crimped pans (pinhole) under nitrogen gas flow, over the temperature range of 25–350 °C, at a 10 °C min^{-1} heating rate. The DSC and TGA curves were obtained on a DSC TA 2920 and on a TGA TA 2920 apparatus, respectively. Data and DTG curves were obtained and processed using the TA Instruments Universal Analysis 2000 software (New Castle, DE). The residual crystallinity of DF in the different samples, expressed as relative degree of crystallinity ($RDC_{\%}$), was determined using the following equation:

$$RDC_{\%} = \Delta H_{sample}/\Delta H_{drug} \times 100 \quad (4)$$

where ΔH_{sample} is the heat of fusion of the sample and ΔH_{drug} is the heat of fusion of the pure crystalline DF, normalized to the drug content in the sample.

2.7. In vitro dissolution studies

The dissolution profiles of pure DF, FDS, and PM in powder were carried out at 37 °C and 100 rpm in a calibrated USP-30 dissolution apparatus 2 (Paddle) (Hanson SR II 6 Flask Dissolution Test Station, Hanson Research Corporation, Chatsworth, CA). The dissolution media consisted in an acid stage for the first 2 h, and a subsequent buffer stage for the next 4 h, in order to mimic the whole gastrointestinal tract fluids, according to *Method A* described in USP-30. The simulated gastric fluid (SGF) was composed of 600 ml, 0.1 N hydrochloric acid solution of pH 1.2. Pure DF, the PM, and FDS were immersed in powder in a 6 mg dose of DF in SGF at time 0, and aliquot (2 ml) samples were collected at 5, 10, 15, 30, 45, 60, 90, and 120 min. Immediately after the 120 min samples were taken, 400 ml of 0.20 M tribasic sodium phosphate was added to the running experiment in SGF to form a pH 6.8 simulated intestinal fluid (SIF), and aliquot (2 ml) samples were withdrawn at 135, 150, 180, 210, 240, 270, 300, and 330 min. All collected samples were filtered through a membrane filter (0.45 μm; nylon filter membrane). An equivalent volume (2 ml) of the corresponding fresh dissolution medium was added to compensate for any loss due to sampling. The concentration of DF was assayed by UV-visible spectrophotometry at 260 nm. The test was repeated three times for each formulation, and the data were reported as a mean ± SD. Sink conditions were maintained at all times. A plot of the cumulative % release of DF against time was constructed to plot the drug release profiles.

3. Results and discussion

3.1. Phase solubility studies

In order to evaluate the formation of binary complexes between DF and βCD, MβCD or HPβCD, and to analyze the effect of these on the aqueous solubility of the drug, phase solubility diagrams of DF in water were obtained, and they are presented in Figure 2. The isotherm of DF can be classified as A-type diagrams for MβCD and HPβCD while for βCD it was B, according to Higuchi and Connors (1965). In the first linear portion of each diagram, it is shown that the aqueous solubility of the drug increases linearly as a function of each ligand concentration, evidencing that water-soluble complexes exist in solution. Besides, the slope values of these first linear portions were less than unity, indicating the formation of 1:1 drug:CD complexes in each range of ligand concentration. The apparent stability constants (K_c), calculated by the Higuchi and Connors equation, for the DF:CD complexes, calculated from the slope of the solubility diagrams, S_{max}, and solubility increments for all the systems are presented in Table 1.

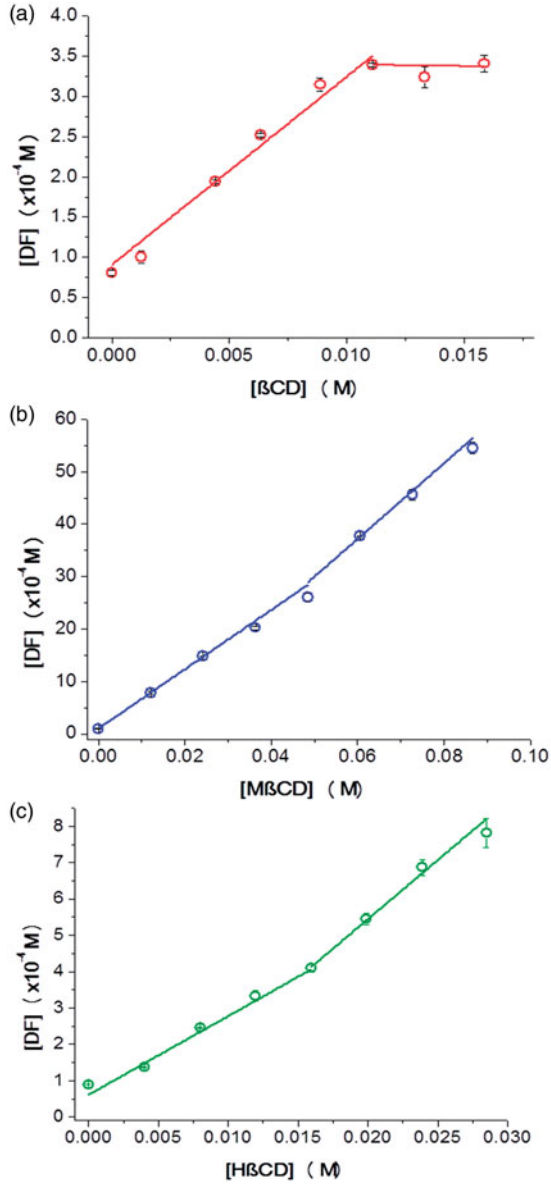

Figure 2. Phase solubility diagrams for DF with: (a) βCD, (b) MβCD, and (c) HPβCD at 25 °C in water.

Table 1. DF solubilities, apparent 1:1 stability constants and solubility increments.

	βCD	MβCD	HPβCD
S_0 DF (mg/ml)		0.029 ± 0.003	
Isotherm type	B_S	A_P	A_P
S_{max} (mg/ml)	0.112 ± 0.003	1.79 ± 0.04	0.26 ± 0.01
SI	3.8 ± 0.4	61 ± 6	8.8 ± 0.9
K_c	268 ± 33	673 ± 71	248 ± 26
CE	8 ± 2	20 ± 4	7 ± 2

S_0: intrinsic solubility of the drug; S_{max}: maximum solubility; K_c: stability constant of the complex; SI: solubility increment; CE: complexation efficiency.

From these values, a different interaction between the drug and the CDs could be deduced. The isotherms of DF with βCD resulted to be B_S-type, where the solubility was increased due to the formation of a soluble complex, and then, at a particular concentration of CD, its maximum solubility was achieved, and remains constant. Previously, Budal et al. described the solubility behavior of the DF:βCD system at pH 7. They also observed an initial linear increment of the DF solubility with βCD concentration, with a stability constant of 427 M^{-1}, and reported that a B_S-type isotherm was obtained, since the solubility decreased due to the reduction in the concentration of free DF in solution, which may have been due to a high concentration of salt in the buffer solution (Budal

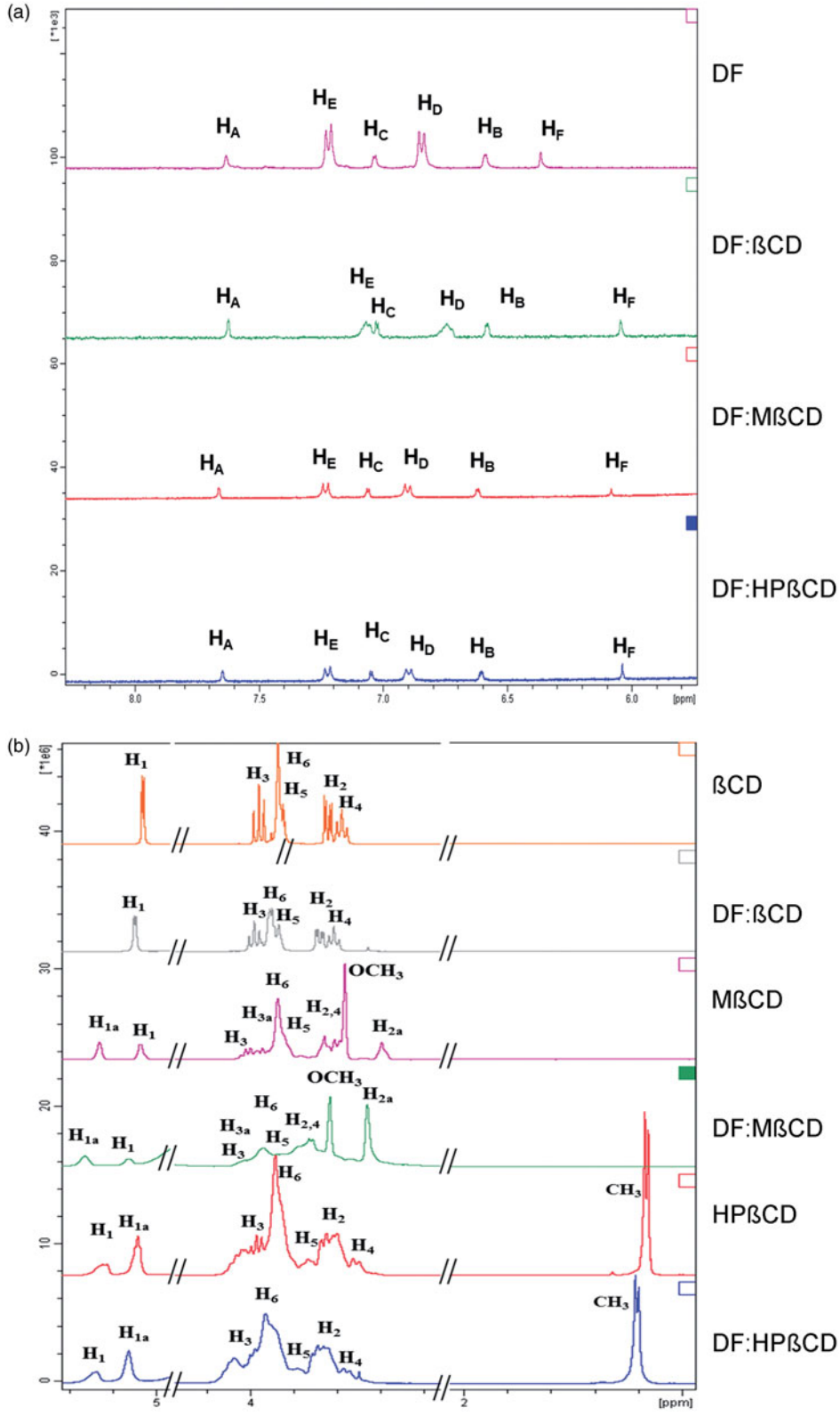

Figure 3. ^{1}H NMR spectra of: (a) pure DF; DF:βCD; DF:MβCD and DF:HPβCD systems in the region of DF signals; and (b) pure βCD; DF:βCD; pure MβCD; DF:MβCD; HPβCD and DF:HPβCD in the regions of CD signals.

et al. 2004). On the other hand, the diagram of DF with MβCD and HPβCD was A_P-type, suggesting an increase in the host–guest ratio at high concentrations of ligand. The highest stability constant and CE were determined for the DF:MβCD system (K_c=673 M^{-1}; CE =20), compared with those of the DF:βCD (K_c=268 M^{-1}; CE =8) and the DF:HPβCD (K_c=248 M^{-1}; CE =7) systems, which were similar between them. Furthermore, the DF:MβCD system showed a 61-fold solubility enhancement of DF in water. According to these results, it was possible to obtain a greater overall solubility by using MβCD as complexation agent, which is related to the higher water solubility of this CD.

3.2. Nuclear magnetic resonance studies

To study the modes of interaction between DF and each of the three CD, the chemical shifts of protons in the pure components and in the binary systems were compared and are presented in Figure 3. The assignments and chemical shifts of the aliphatic βCD, MβCD, and HPβCD protons and the aromatic DF protons measured in D_2O before and after complexation are listed in Table 2. For βCD (Aloisio et al. 2014), MβCD (Delrivo et al. 2012), and HPβCD (Loukas et al. 1996), assignments of peaks to protons were performed following previous publications (Table 2(a)). The magnitude of the H_5 and H_3 shifts can be used as a measure of the complex stability as well as of the depth of inclusion (Rekharsky et al. 1995). Thus, in this study, for the complexes with MβCD, the most significant upfield shifts were observed for the inner cavity CD protons H_5 and H_3, and a downfield displacement was observed for H_6 proton, extending from the narrow rim of the CD cavity, and for the proton located in the $0CH_3$ moiety of MβCD. The system with HPβCD exhibited downfield displacements not only for the inner cavity CD protons H_3 and H_5, but also for the protons at the outer surface of the CD torus (H_1 and H_{1a}). Besides, a downfield displacement was observed for H_6 proton. On the other hand, the complex with βCD showed the highest downfield shifts for protons at the outer surface of the CD torus (H_1, H_2, H_4, and H_6). In addition, upfield displacements were observed for most of DF protons in the DF:βCD system, except for the G proton for which a downfield displacement was observed. Moreover, upfield shifts could be observed for the H_F proton for the DF in the systems with MβCD and HPβCD, and downfield

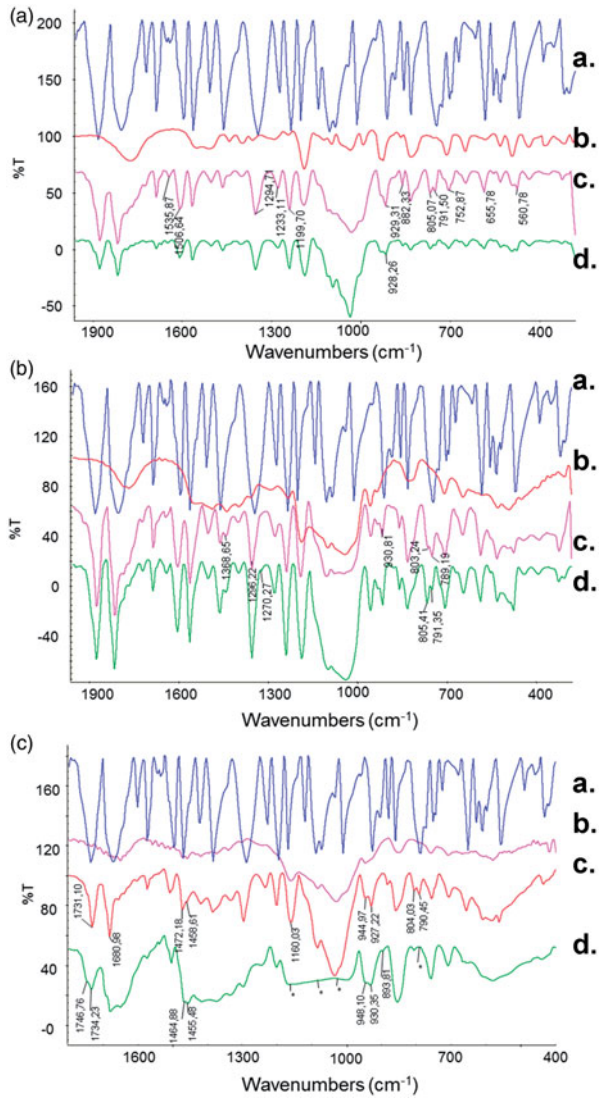

Figure 4. FT-IR spectra of: (a) pure DF; (b) pure CD; (c) PM, and (d) FDS for: (a) DF:βCD; (b) DF:MβCD, and (c) DF:HPβCD systems.

Table 2. Chemical shifts. (a) DF in the presence of βCD, MβCD or HPβCD.

	δ DF	δ DF:βCD	Δδ	δ DF:MβCD	Δδ	δ DF:HPβCD	Δδ
H_A	7.633	7.619	−0.014	7.657	0.024	7.643	0.010
H_B	6.594	6.58	−0.014	6.619	0.025	6.606	0.012
H_C	7.035	7.018	−0.017	7.0595	0.0245	7.041	0.006
H_D	6.846	6.741	−0.105	6.8985	0.053	6.8955	0.05
H_E	7.2200	7.064	−0.156	7.2295	0.0095	7.2215	0.0015
H_F	6.367	6.042	−0.325	6.08	−0.287	6.035	−0.332
H_G	3.326	3.455	0.129	3.459	0.133	3.497	0.171

(b) CDs in the presence of DF

	δ βCD	δ DF:βCD	Δδ	δ MβCD	δ DF:MβCD	Δδ	δ HPβCD	δ DF:HPβCD	Δδ
H_1	5.0678	5.0975	0.0297	5.2507	5.328	0.0773	5.2517	5.285	0.0333
H_{1a}	–	–	–	5.0638	5.129	0.0652	5.0978	5.128	0.0302
H_2	3.647	3.678	0.031	Overlapped with H_4	[b]	–	3.6489	3.613	−0.0359
H_{2a}	–	–	–	3.3841	[b]	–	–	–	–
H_3	3.9654	3.979	0.0136	4.0081	3.776	−0.2321	3.9839	4.076	0.0921
H_{3a}	–	–	–	3.9284	3.94	0.0116	–	–	–
H_4	3.5835	3.612	0.0285	Overlapped with H_2	[b]	–	3.5214	3.5205	−0.0009
H_5	3.8505	3.867	0.0165	3.6698	3.459	−0.2108	3.7454	3.779	0.0336
H_6	3.8774	3.9025	0.0251	3.8624	4.03	0.1676	3.8947	3.93	0.0353
OCH_3	–	–	–	3.5518	3.717	0.1652	–	–	–

[a]Methylated position.
[b]Undistinguishable.

displacements for the A, B, C, and D protons for the DF:MβCD system, probably due to van der Waals interactions between the drug and the hydrophobic inner side of CD (Anguiano-Igea et al. 1997). The most marked downfield displacements corresponded to H_F in the three systems, which is geminal to the two chloride substituent. Therefore, the lowest electron density gives them a greater affinity for the inner CD cavity. These findings support an external interaction of the drug with βCD, the full inclusion of DF inside the MβCD cavity, and the partial inclusion in HPβCD. The benzene and the alkyl moiety with the chloride substituent may be the groups involved in the external interaction with βCD and were partially included in HPβCD.

3.3. Fourier-transform infrared spectroscopy

FT-IR spectroscopy was used to assess the interaction between DF and each CD in the solid state, because the changes in the shape, shift, and intensity of the IR absorption peaks of the guest or host can provide enough information for the occurrence of the inclusion. The FT IR spectra of pure substances, FDS and PM of DF with βCD, MβCD, or HPβCD are presented in Figure 4. In the DF:βCD PM, the C–Cl stretching signals of DF (879 and 858 cm^{-1}) were shifted to lower frequencies (805 and 791 cm^{-1}) and the signals corresponding to the CO–O stretching band of the ester group in DF:βCD PM (1294, 1233, and 1199 cm^{-1}) were shifted to higher frequencies in the FDS, and in this last system, the aromatic ring vibration signals (1571 and 1600 cm^{-1}) were shifted to lower frequencies (1506 and 1535 cm^{-1}). Besides, the C–H out of plane vibration peaks of DF (924 and 903 cm^{-1}) presented their relative intensities modified.

On the other hand, in the DF:MβCD PM the signals corresponding to the CO–O stretching band of the ester group of DF presented shifts to higher frequencies (1296 and 1368 cm^{-1}), whereas that the intensity relations of the C–Cl stretching signals of DF (879 and 858 cm^{-1}) were modified (803 and 789 cm^{-1}). In the DF:MβCD FDS, a new signal appeared at 1270 cm^{-1}.

On the other hand, in the DF:HPβCD FDS, the C=O stretching band of the lactone moiety of DF (1670 cm^{-1}) was shifted to a higher frequency (1680 cm^{-1}) in comparison with the PM and a new signal appeared at 1746 cm^{-1}. Furthermore, the aromatic ring vibration signals (1571 and 1600 cm^{-1}) presented their intensity relations modified. Besides, the C–H out of plane vibration peaks of DF (924 and 903 cm^{-1}) were broadened. Added to the above, the signals of the C–Cl stretching of DF (879 and 858 cm^{-1}) appeared in DF:HPβCD PM and were absent in the FDS.

According to these observations, it can be stated that the changes in DF:βCD PM and DF:MβCD PM indicated the presence of interactions between the components, but with not enough evidence to confirm the formation of complexes. On the other hand, the differences between the PM and the PDS profiles may suggest the formation of true complexes of DF with βCD, MβCD, and HPβCD when they are prepared by means of lyophilization.

3.4. Differential scanning calorimetry and thermogravimetric analysis

In order to evaluate the formation of inclusion binary complexes, the thermal behavior of pure substances, FDS and PM of DF with βCD, MβCD, or HPβCD in the solid state, was monitored by DSC, TGA, and DTG curves, which are illustrated in Figure 5. The DF thermal curve was typical of a crystalline substance and was

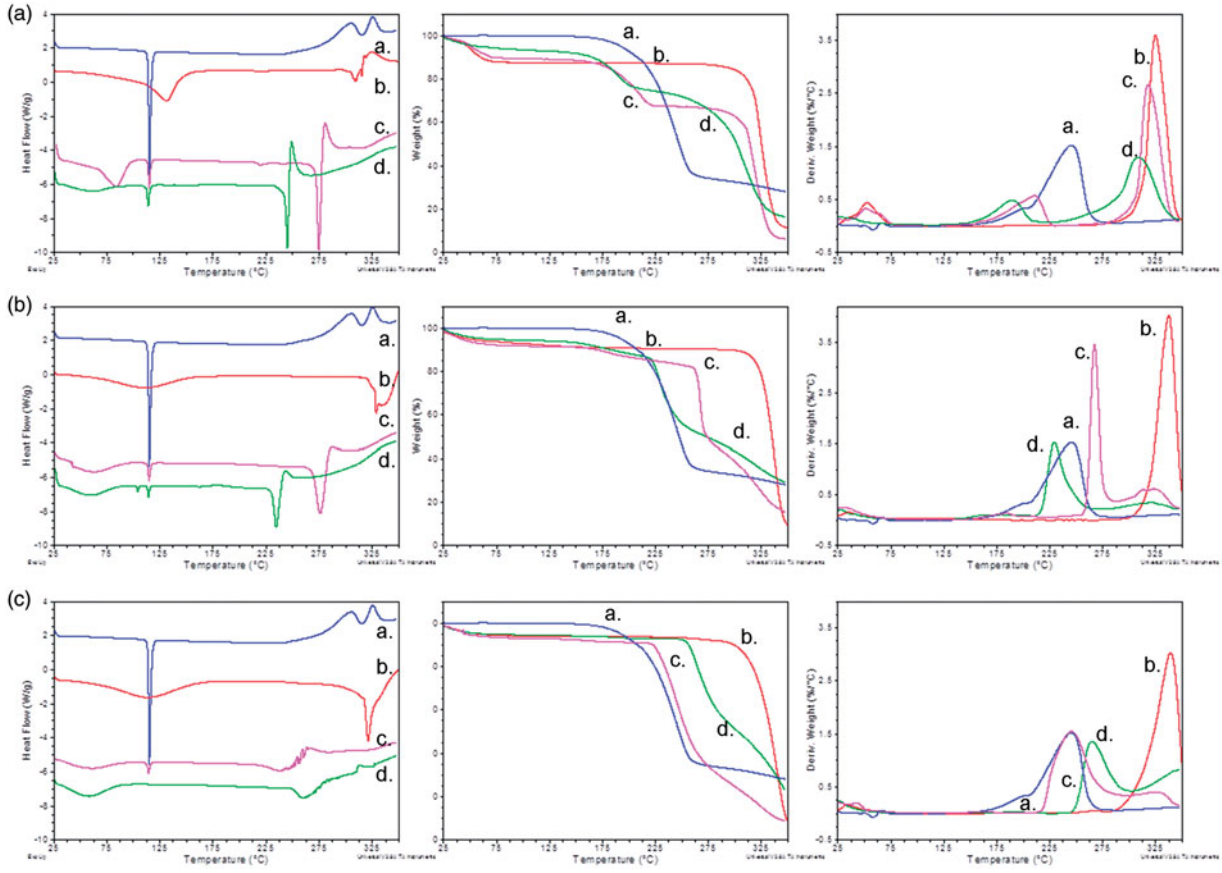

Figure 5. DSC, TGA, and DTG curves of: (a) pure DF; (b) pure CD; (c) PM, and (d) FDS for: (a) DF:βCD; (b) DF:MβCD, and (c) DF:HPβCD systems.

characterized by a sharp endothermic peak (at 115.01 °C), assigned to its melting point, and decomposing above 250 °C. As it can be observed by a comparison of the TGA and DSC curves, CD lost water at temperatures in the range from 25 to 150 °C and decomposed above 250 °C, as evidenced by the mass loss in the TGA curves. The endothermic peaks due to melting of the drug were present in the PM of DF with βCD (114.83 °C), MβCD (114.73 °C), and HPβCD (114.73 °C), whereas that the $RDC_{\%}$ values were 19, 13, and 10, respectively. In addition, these curves exhibited shifts on temperature and changes in mass loss corresponding to the dehydration event of CD. These events could be explained by the weak molecular interactions between the DF and CD at high temperatures, but these were not evidence of the formation of true inclusion compounds. On the other hand, all the lyophilized samples presented shifts on the corresponding CD dehydration temperature and DF:βCD and DF:MβCD FDS also presented changes in the decomposition profiles. In addition, the melting peak of free DF was small in the DSC curves of the DF:HPβCD FDS, with a RDC% value of 1%. An additional sharp peak at 104.03 °C, next to the melting peak at 114.73 °C ($RDC_{\%} = 4\%$), was present in the FDS with MβCD ($RDC_{\%} = 7\%$). We suggest that these events may be related to the melting of the released drug from the inclusion complex after the dehydration of MβCD, followed by the melting of non-included drug. In accordance to this, the DTG curve of the DF:βCD FDS presented two decomposition events, and only the one at higher temperatures, which can be ascribed to non-included drug, resembles with the endotherm of pure DF. On the contrary, in the DF:βCD FDS, the endothermic peaks, due to melting of the drug, was present (114.07 °C), with a $RDC_{\%}$ value of 17%, and the decomposition profile is quite similar to the PM. These results may suggest the formation of true inclusion complexes of DF only with MβCD and HPβCD and when they were prepared by means of lyophilization, in accordance to the observed events, mainly represented by the shifts on the corresponding CD dehydration temperature and changes in the decomposition profiles, that in comparison with the corresponding PM, are evidence of complexation and not only weak molecular interactions at high temperatures. In addition, the $RDC_{\%}$ values in the PM with MβCD and HPβCD (13 and 10) were substantially diminished in the FDS (4 and 1), indicating that the crystallinity of the drug was reduced by the incorporation in the complexes.

3.5. In vitro-*dissolution studies*

The effect of βCD, MβCD, and HPβCD on the dissolution behavior of DF was tested, and the results are presented in Figure 6. It can be seen that the dissolution of DF in SGF was linear and fast, attaining a 43% of drug dissolved in 2 h. On the contrary, the dissolution in SIF was slow, with a 27% increment with respect to the already dissolved drug in the SGF, attaining a 70% of the dissolved drug at 150 min. All the PM profiles displayed no significant differences compared with those of the plain drug, indicating that no benefit in terms of dissolution rate enhancement exists by the simple mixing of the components. On the other hand, the dissolution of DF in the FDS with βCD, MβCD, and HPβCD presented 85; 77 and 75% of dissolved drug at 5 min, respectively. The dissolution in SGF from the three FDS reaches the 100% of the dissolved drug at 150 min. Moreover, no precipitation of the drug was observed when the media was changed to SIF. These results demonstrated an increased dissolution rate of DF from the FDS in comparison to the free drug and the PM, suggesting the formation of inclusion complexes of DF with solubilities higher than the plain drug, when the complexes were obtained by the freeze-dry technique.

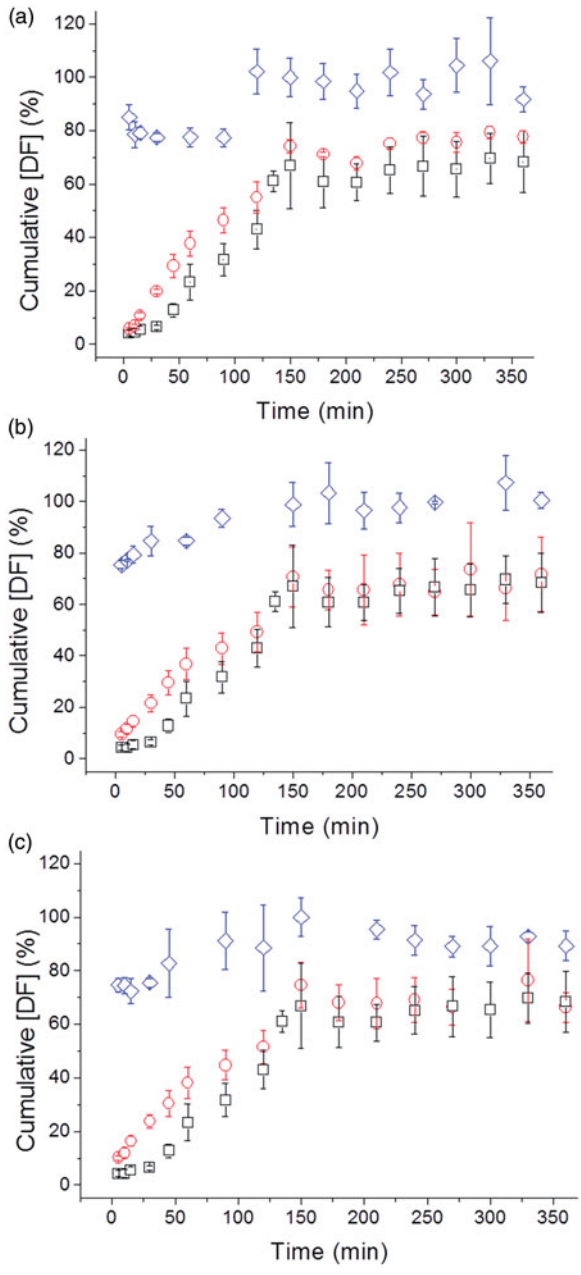

Figure 6. Dissolution profiles of: Pure DF (□); PM (○), and FDS (◇) of: (a) DF:βCD, (b) DF:MβCD, and (c) DF:HPβCD systems (each value represents the mean ± SD of $n \geq 3$).

4. Conclusions

Phase solubility studies indicated the formation of 1:1 drug:CD complexes at low concentrations of ligand, and the highest stability constant and solubility enhancement was determined for the DF:MβCD system. NMR experiments demonstrated the inclusion of DF into the CD cavity of MβCD and HPβCD, and an exclusion complex with βCD. Also, the differences between the PM and the FDS FT IR and thermal analysis profiles suggested the formation of genuine inclusion complexes of DF with MβCD and HPβCD and an exclusion complex with βCD when they are prepared by means of lyophilization. It is worth highlighting that characterization studies that confirm the formation of a complex between DF and

βCD, MβCD, or HPβCD have been poor so far with regard to DF:CD complexes. In this work the mode interactions of DF with βCD, MβCD, and HPβCD were successfully determined, and solid state characterization of DF:CD complexes was properly performed. Besides, *in vitro* dissolution studies, conducted in SGF followed by SIF, provided a comprehensive perspective of the dissolution behavior of the drug in the gastrointestinal tract. It was demonstrated that the complexation with βCD, MβCD, and HPβCD resulted in an increased dissolution rate of DF from the FDS, suggesting the formation of complexes with solubilities higher than the plain drug. This fact is substantially important to avoid the precipitation of DF in the intestinal lumen, since this is the site of infection of *Entamoeba histolytica*; full bioavailability of the drug is needed to achieve the therapeutic effectiveness.

Acknowledgements

Dr Gloria M. Bonetto's assistance and her helpful discussion in NMR measurements is highly appreciated. We also want to thank Ferromet S.A. (Roquette's agent in Argentina) for their donation of cyclodextrins.

Disclosure statement

The authors report no conflicts of interest.

Funding

The authors wish to acknowledge the support from the Consejo Nacional de Investigaciones Científicas y Técnicas (CONICET) and the Universidad Nacional de Córdoba, both of which provided grants and facilities for this investigation. Financial support from 'Fondo para la Investigación Científica y Tecnológica' (FONCYT) Préstamo BID PICT 2012-1461 and 'Secretaría de Ciencia y Técnica de la Universidad Nacional de Córdoba' (SECyT-UNC), is greatly acknowledged.

References

Aloisio C, Gomes de Oliveira A, Longhi M. 2014. Characterization, inclusion mode, phase-solubility and in vitro release studies of inclusion binary complexes with cyclodextrins and meglumine using sulfamerazine as model drug. Drug Dev Ind Pharm. 40:919–928.

Anguiano-Igea S, Otero-Espinar FJ, Vila-Jato JL, Blanco-Méndez J. 1997. Interaction of clofibrate with cyclodextrin in solution: phase solubility, 1H NMR and molecular modelling studies. Eur J Pharm Sci. 5:215–221.

Araújo MV, Barbosa EK, Lázaro G, Conegero LS, Almeida LE, Barreto LS, da Costa NB, Gimenez IF. 2008. Sulfadiazine/hydroxypropyl-β-cyclodextrin host-guest system: characterization, phase-solubility and molecular modeling. Bioorg Med Chem. 16:5788–5794.

Barillaro V, Dive G, Bertholet P, Evrard B, Delattre L, Frederich M, Ziémons E, Piel G. 2007. Theoretical and experimental investigations of organic acids/cyclodextrin complexes and their consequences upon the formation of miconazole/cyclodextrin/acid ternary inclusion complexes. Int J Pharm. 347:62–70.

Blanco-García E, Guerrero-Callejas F, Blanco-Méndez J, Gómez-Couso H, Luzardo-Álvarez A. 2016. Development of particulate drug formulation against *C. parvum*: formulation, characterization and in vivo efficacy. Eur J Pharm Sci. 92:74–85.

Brewster ME, Loftsson T. 2007. Cyclodextrins as pharmaceutical solubilizers. Adv Drug Deliv Rev. 59:645–666.

Budal RM, Da Graça Nascimento M, Dal Magro J, Vázquez tato J, Yunes RA. 2004. Studies on the inclusion complex of diloxanide furoate-β-cyclodextrin. J Incl Phenom Macrocycl Chem. 50:151–155.

Castro Hermida JAA, Ares-Mazás MEE, Otero Espinar F, Blanco Méndez J. 2001. Inhibition of Cryptosporidium infection in mice treated with a cyclodextrin inclusion complex with diloxanide furoate. Parasitol Res. 87:449–452.

Delrivo A, Zoppi A, Longhi MR. 2012. Interaction of sulfadiazine with cyclodextrins in aqueous solution and solid state. Carbohydr Polym. 87:1980–1988.

Duchêne D, Bochot A. 2016. Thirty years with cyclodextrins. Int J Pharm. 514:58–72.

Farthing MJG. 2006. Treatment options for the eradication of intestinal protozoa. Nat Clin Pract Gastroenterol Hepatol. 3:436–445.

García A, Leonardi D, Vasconi MD, Hinrichsen LI, Lamas MC, Deli MA. 2014. Characterization of albendazole-randomly methylated-β-cyclodextrin inclusion complex and in vivo evaluation of its antihelmitic activity in a murine model of Trichinellosis. PLoS One. 9:e113296.

Garnero C, Longhi M. 2007. Study of ascorbic acid interaction with hydroxypropyl-β-cyclodextrin and triethanolamine, separately and in combination. J Pharm Biomed. 45:536–545.

Granero GE, Maitre MM, Garnero C, Longhi MR. 2008. Synthesis, characterization and in vitro release studies of a new acetazolamide–HP-β-CD–TEA inclusion complex. Eur J Med Chem. 43:464–470.

Higuchi T, Connors K. 1965. Phase solubility techniques. In: Reilly CW, editor. Advances in analytical chemistry and instrumentation. New York (NY): Wiley-Interscience; p. 117–212.

Kutyła MJ, Lambert LK, Davies NM, McGeary RP, Shaw PN, Ross BP. 2013. Cyclodextrin-crosslinked poly(acrylic acid): synthesis, physicochemical characterization and controlled release of diflunisal and fluconazole from hydrogels. Int J Pharm. 444:175–184.

Loukas YL, Vraka V, Gregoriadis G. 1996. Use of a nonlinear least-squares model for the kinetic determination of the stability constant of cyclodextrin inclusion complexes. Int J Pharm. 144:225–231.

Mishal A, Sober D. 2005. Stability indicating reversed-phase liquid chromatographic determination of metronidazole benzoate and diloxanide furoate as bulk drug and in suspension dosage form. J Pharm Biomed Anal. 39:819–823.

Mora MJ, Longhi MR, Granero GE. 2010. Synthesis and characterization of binary and ternary complexes of diclofenac with a methyl-β-CD and monoethanolamine and in vitro transdermal evaluation. Eur J Med Chem. 45:4079–4088.

Ojarinta R, Heikkinen AT, Sievänen E, Laitinen R. 2017. Dissolution behavior of co-amorphous amino acid-indomethacin mixtures: the ability of amino acids to stabilize the supersaturated state of indomethacin. Eur J Pharm Biopharm. 112:85–95.

Onnainty R, Longhi MR, Granero GE. 2011. Complex formation of chlorhexidine gluconate with hydroxypropyl-β-cyclo-dextrin (HP-β-CD) by proton nuclear magnetic resonance spectroscopy (1H NMR). Carbohydr Res. 346:1037–1046.

Özdemir N, Erkin J. 2012. Enhancement of dissolution rate and bioavailability of sulfamethoxazole by complexation with β-cyclodextrin. Drug Dev Ind Pharm. 38:331–340.

Piel G, Piette M, Barillaro V, Castagne D, Evrard B, Delattre L. 2006. Betamethasone-in-cyclodextrin-in-liposome: the effect of cyclodextrins on encapsulation efficiency and release kinetics. Int J Pharm. 312:75–82.

Rekharsky MV, Goldberg RN, Schwarz FP, Tewari YB, Ross PD, Yamashoji Y, Inoue Y. 1995. Thermodynamic and nuclear magnetic resonance study of the interactions of α- and β-cyclodextrin with model substances: phenethylamine, ephedrines, and related substances. J Am Chem Soc. 117:8830–8840.

Ribeiro L, Ferreira D, Veiga F. 2003. Physicochemical investigation of the effects of water-soluble polymers on vinpocetine complexation with beta-cyclodextrin and its sulfobutyl ether derivative in solution and solid state. Eur J Pharm Sci. 20:253–266.

Taupitz T, Dressman JB, Buchanan CM, Klein S. 2013. Cyclodextrin-water soluble polymer ternary complexes enhance the solubility and dissolution behaviour of poorly soluble drugs. Case example: itraconazole. Eur J Pharm Biopharm. 83:378–387.

Veiga F, Pecorelli C, Ribeiro L. 2006. As ciclodextrinas em tecnología farmacéutica. Coimbra: Minerva Coimbra.

Yi L, Zhang T, Tao J, Ji G, Wang S. 2009. Preparation, characterization, and pharmacokinetics of the inclusion complex of genipin-β-cyclodextrin. Drug Dev Ind Pharm. 35:1452–1459.

Zoppi A, Garnero C, Linck YG, Chattah AK, Monti GA, Longhi MR. 2011. Enalapril:β-CD complex: stability enhancement in solid state. Carbohydr Polym. 86:716–721.